Supporting Information

Nobori et al. 10.1073/pnas.1800529115

A

	Bacteria CDS	Bacteria non-coding	Plant	Else
rRNA depletion (Bacteria) only (n = 3)	0.18%	0.58%	78.30%	20.94%
rRNA depletion (Plant & Bacteria) only (n = 3)	0.58%	0.27%	86.87%	12.28%
Bacteria enriched (n = 100)	19.14%	8.26%	55.86%	16.74%

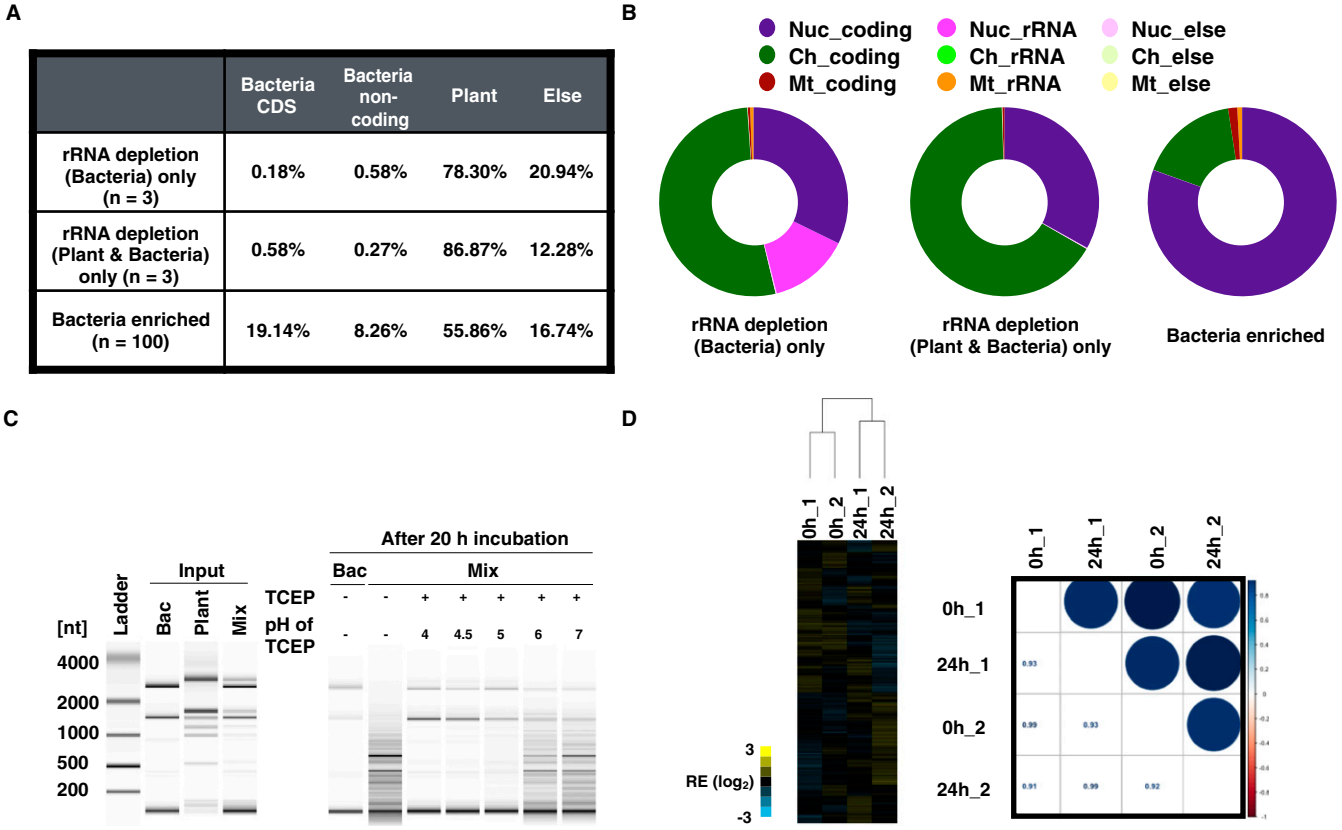

Fig. S1. Bacterial enrichment and quality of RNA extraction in the *in planta* bacterial transcriptome. (*A*) Proportion of the sequencing reads mapped on the *Pto* (Bacteria) CDS, the *Pto* noncoding sequence, the *A. thaliana* (Plant) genome, and on neither the *Pto* nor the *A. thaliana* genome (Else). (*B*) Proportion of the RNA-seq reads mapped on the *A. thaliana* genome. (*Left* and *Middle*) RNA extracted from the infected leaves, followed by bacterial rRNA depletion only (*Left*) and by bacterial and plant rRNA depletion (*Middle*) ($n = 3$). (*Right*) RNA extracted from the bacteria-enriched samples, followed by bacterial and plant rRNA depletion (Bacteria enriched; $n = 8$; a subset of all 100 *in planta* samples was randomly selected). Protein coding RNA (coding), ribosomal RNA (rRNA), and other RNA (else) encoded in the nucleus (Nuc), chloroplast (Ch), and mitochondrion (Mt) is shown. (*C*, *Left*) Assessment of RNA integrity with the 2100 Bioanalyzer (Agilent). Total RNA from *Pto* (Bac.), *A. thaliana* leaves (Plant), and the mixture of both (Mix) was analyzed. (*Right*) Bacterial cells were incubated with crushed *A. thaliana* leaves in RNA-stabilizing buffer (9.5% ethanol and 0.5% phenol) without or with TCEP at different pHs for 20 h at 4 °C. Then total RNA was extracted and analyzed. (*D*) Bacterial isolation buffer fixes the bacterial transcriptome. *Pto* ($OD_{600} = 0.65$) was incubated in bacterial isolation buffer for 0 h or 24 h, followed by RNA extraction and RNA-seq. Hierarchical clustering (*Left*) and Pearson correlation (*Right*) plots of all genes detected are shown ($n =$ 2 biological replicates from two independent experiments). RE, relative expression.

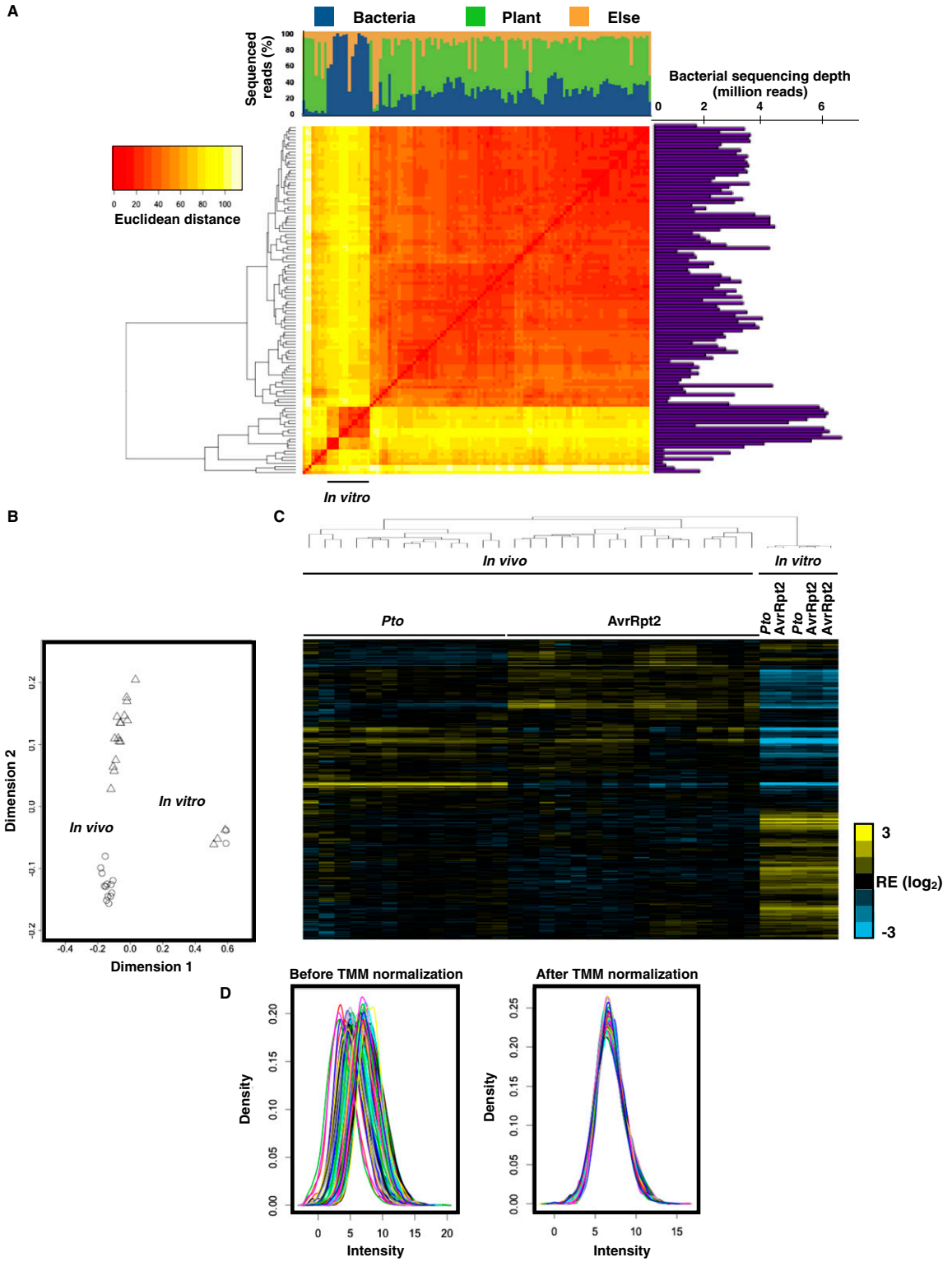

Fig. S2. Normalization and quality control of RNA-seq data. (*A*, *Upper*) The ratio of sequencing reads mapped on the bacterial genome (blue), plant genome (green), and on neither the bacterial nor the plant genome (Else) (orange) in each sample. (*Lower Left*) Heatmap of Euclidean distances between RNA-seq data of each sample. (*Lower Right*) Sequencing depth of bacterial RNA in each sample. (*B*) MDS plot of the RNA-seq data of *Pto* (circles) and *Pto* AvrRpt2 (triangles) profiled in in vivo (Col-0) and in vitro (King's B medium) conditions. Distances represent leading $\log_2$-fold differences between samples. (*C*) Hierarchical clustering of the relative expression (RE) of the RNA-seq data of *Pto* and *Pto* AvrRpt2 profiled in in vivo (Col-0) and in vitro (King's B medium) conditions. (*D*) Density plots of $\log_2$-transformed count per million RNA-seq data (Intensity) before (*Left*) and after (*Right*) TMM normalization. All 114 samples were plotted.

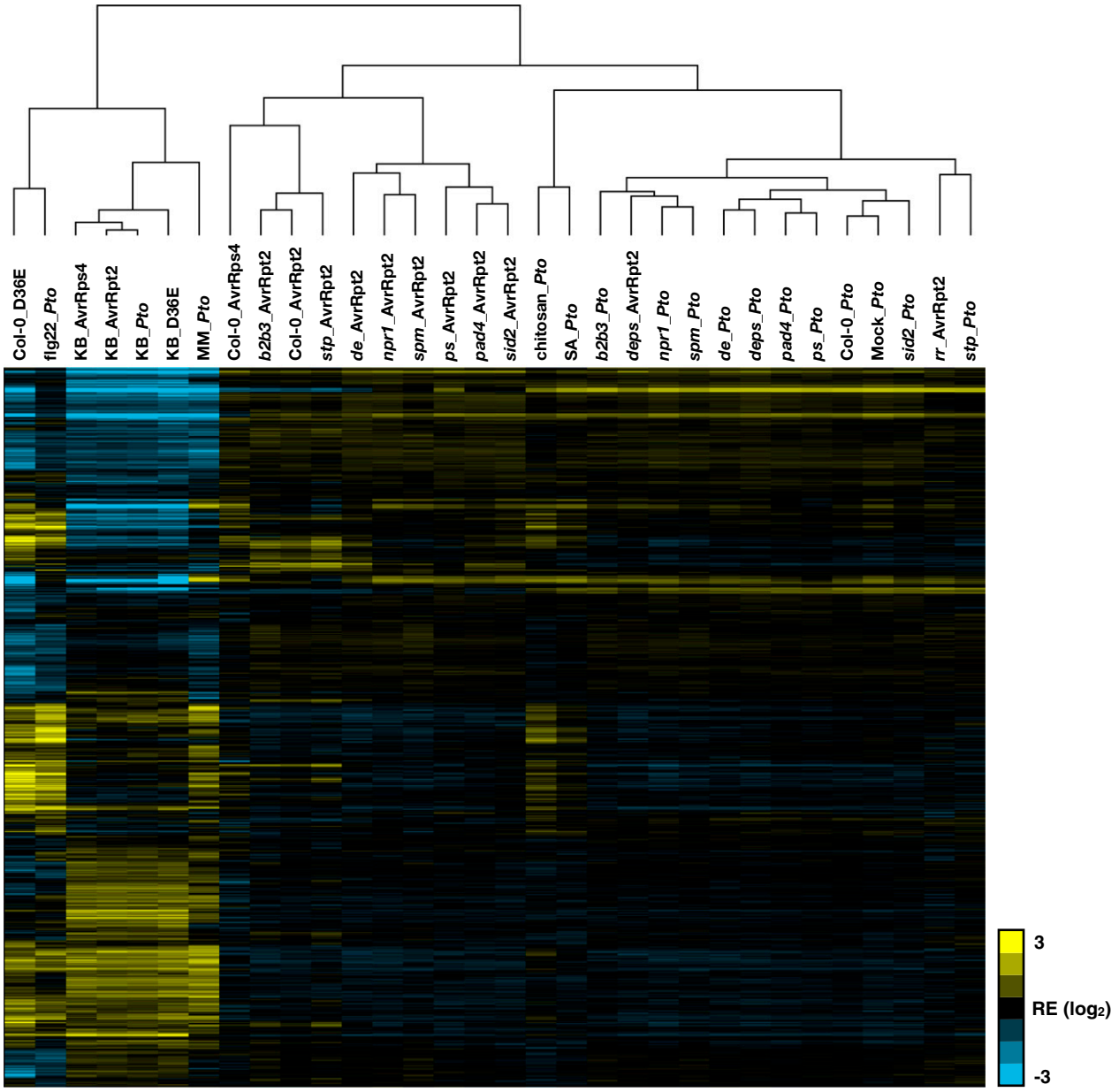

Fig. S3. Heatmap of the relative expression (RE) of *Pto* transcriptomes in all samples analyzed in this study. Hierarchical clustering was performed for both the genes (rows) and the samples (columns). The sample name consists of the name of the bacterial strain preceded by the name of host genotype, pretreatments to Col-0, or in vitro conditions (see Fig. 2*A* for the acronyms and Dataset S6 for the mean expression values).

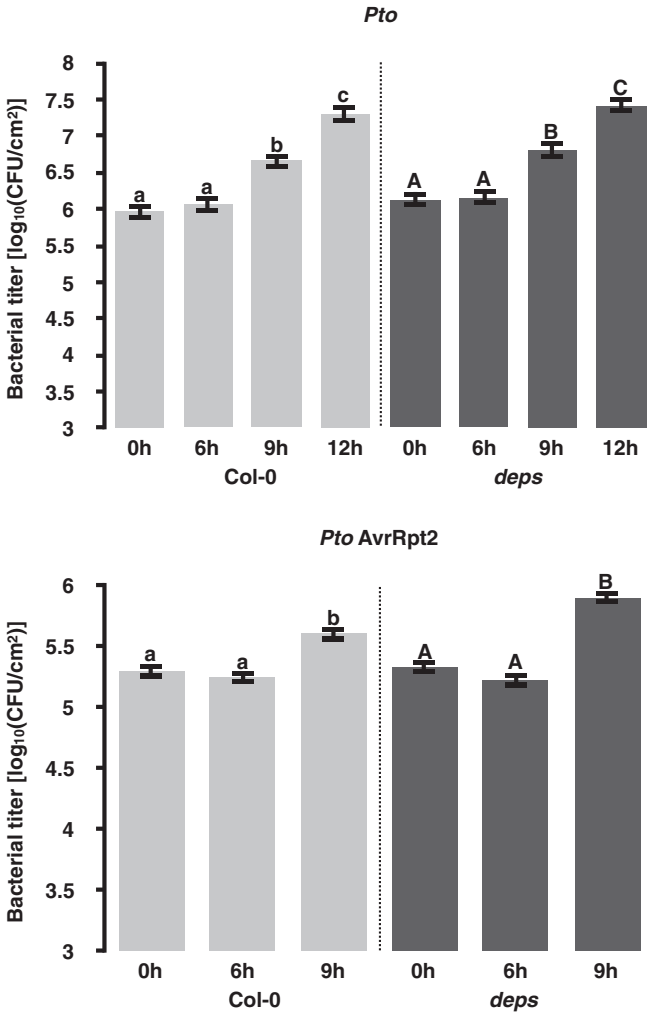

Fig. S4. *Pto* populations did not change at 6 hpi. Growth assay of *Pto* (*Upper*) or *Pto* AvrRpt2 (*Lower*) in Col-0 and *dde2 ein2 pad4 sid2* (*deps*) plants at the indicated time points. The bacterial suspension (OD_{600} = 0.5) was syringe infiltrated into leaves. Means ± SEM were calculated using the mixed linear model (n = 24 biological replicates from two independent experiments). Different letters indicate statistically significant differences in each genotype (adjusted P < 0.001; Benjamini–Hochberg method).

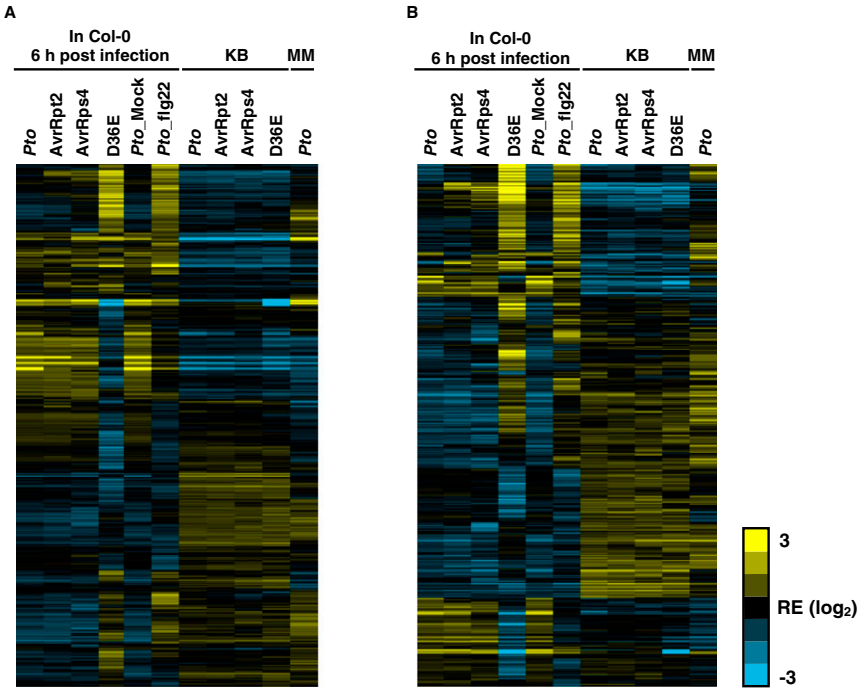

Fig. S5. Profiles of the *Pto* transcriptome under various conditions. (*A*) Hierarchical clustering of the relative expression (RE) of 3,344 genes detected in all samples. (*B*) Hierarchical clustering of the RE of genes annotated as "hypothetical protein" that were differentially regulated in at least one of the comparisons shown in Fig. 2*C*.

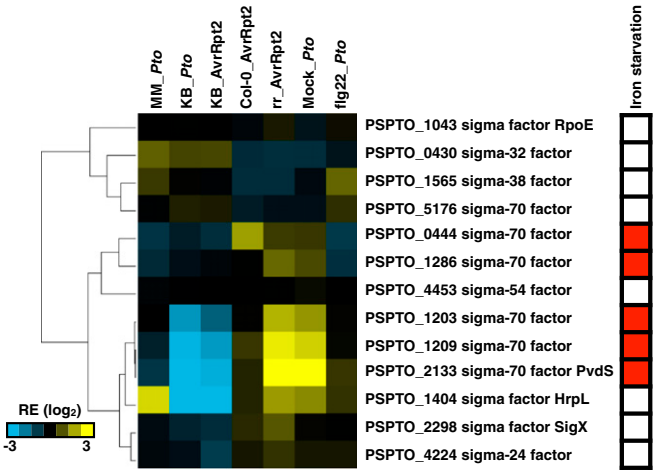

Fig. S6. Hierarchical clustering of the relative expression (RE) of *Pto* sigma factors. The red squares show the iron-starvation–related sigma factors (1). KB, King's B medium; MM, minimal medium; *rr*, *rps2 rpm1*.

1. Markel E, et al. (2013) Regulons of three Pseudomonas syringae pv. tomato DC3000 iron starvation sigma factors. *Appl Environ Microbiol* 79:725–727.

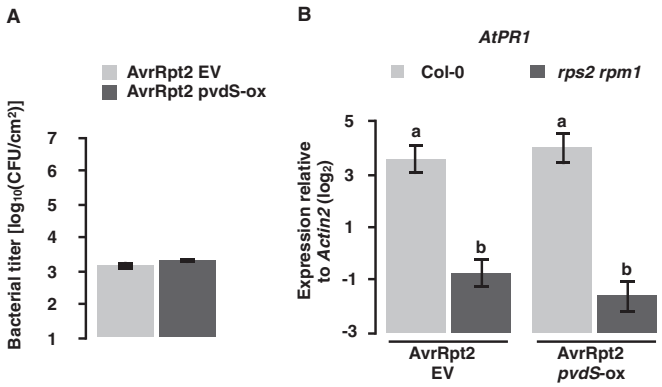

Fig. S7. Infection assay of *pvdS*-overexpressing *Pto*. (*A*) Growth assay of *Pto* AvrRpt2 (EV) and *Pto* AvrRpt2 *pvdS*-ox (OD_{600} = 0.001) in Col-0 and *rps2 rpm1* plants at 0 h hpi. (*B*) RT-qPCR analysis of *PR1* expression in Col-0 and *rps2 rpm1* plants infected with *Pto* AvrRpt2 (EV) or *Pto* AvrRpt2 *pvdS*-ox (OD_{600} = 0.001) at 24 hpi. Mean ± SEM was calculated using a mixed linear model (*A*: n = 52 biological replicates from six independent experiments; *B*: n = 2 biological replicates from two independent experiments). Different letters indicate statistically significant differences (adjusted $P < 0.05$; Benjamini–Hochberg method).

Other Supporting Information Files

Dataset S1 (XLSX)
Dataset S2 (XLSX)
Dataset S3 (XLSX)
Dataset S4 (XLSX)
Dataset S5 (XLSX)
Dataset S6 (XLSX)
Dataset S7 (XLSX)
Dataset S8 (XLSX)